

Step by Step: Using Step Selection Analysis to Simulate Dispersal and Assess Landscape Connectivity

David D. Hofmann^{1,§} John W. McNutt² Arpat Ozgul¹ Gabriele Cozzi^{1,2}
Dominik M. Behr^{1,2}

May 5, 2021

¹ Department of Evolutionary Biology and Environmental Studies, University of Zurich,
Winterthurerstrasse 190, 8057 Zurich, Switzerland.

² Botswana Predator Conservation, Private Bag 13, Maun, Botswana.

§ Corresponding author (david.hofmann2@uzh.ch)

Running Title: Release the Dogs! Simulating Wild Dog Dispersal to Assess Landscape
Connectivity

Keywords: dispersal, simulation, movement, integrated step selection, Kavango-Zambezi
Transfrontier Conservation Area, landscape connectivity, *Lycaon pictus*

Abstract

Dispersal is an important process that allows species to avoid inbreeding, to colonize new habitats and to reinforce non-viable subpopulations. Successful dispersal thus represents a crucial pre-requisite for long-term species persistence in wild animal populations. However, the ability to disperse is contingent a sufficient degree of landscape connectivity, which is why the estimation of connectivity and identification of dispersal corridors has become a task of extraordinary importance in ecological studies.

Over the past two decades, ecologists have primarily relied on analytical tools such as least-cost methods and circuit theory to investigate landscape connectivity. Despite their usefulness for various ecological applications, both methods make several restricting assumptions that limit their suitability in reality. To address their shortcomings, simulations from individual-based movement models have been proposed and applied. To overcome their shortcomings, simulations from individual-based movement models have been proposed. Yet, due to the infinite number of possibilities of coming up with an individual-based model, a unified and objective framework is missing.

Recent innovations in movement ecology have brought forward novel opportunities to study animal dispersal and landscape connectivity. In particular, the rich suite of resource selection functions, including point-, step-, and path-selection functions have undergone substantial improvements over the past years. Most notably, step-selection functions have been generalized to *integrated* step selection functions, which essentially represent fully mechanistic movement models based on which individual animal movement could be simulated. While such models have been applied to study *steady-state* utilization distribution, a similar approach may be useful for investigating *transient* movement behavior and thereby study landscape connectivity by means of simulated dispersal events.

Here, we showcase the use of integrated step selection analysis to simulate dispersal of the highly endangered African wild dog across the world's largest transboundary conservation area, the Kavango-Zambezi Transfrontier Conservation Area (KAZA-TFCA). For this, we utilize data collected on 16 dispersing wild dog coalitions departing from northern Botswana. We combine the movement data with relevant spatial covariate layers and used integrated step selection functions to parametrize a fully mechanistic movement model rendering wild dog dispersal. Based on this model, we simulate 80'000 dispersers, originating from protected areas and moving across the extent of the KAZA-TFCA. We then generate a heatmap and use network theory to reveal dispersal hotspots and crucial bottlenecks across the study area. Finally, we discuss the benefits and pitfalls of such dispersal simulations and highlight potential improvements to be made in the future.

Contents

1	Introduction (90%)	1
1.1	Importance of Dispersal & Connectivity (90%)	1
1.2	Advancements in GPS Technology & Movement Ecology (90%)	1
1.3	Resource Selection & Connectivity (90%)	1
1.4	Issues with Least-Cost Paths & Circuit Theory (90%)	2
1.5	What about IBMMs? (90%)	3
1.6	Step Selection Analysis (90%)	3
1.7	Study Species & Study Area (90%)	4
1.8	Previous Paper (90%)	4
2	Methods	5
2.1	Study Area (90%)	5
2.2	GPS Relocation Data (90%)	5
2.3	Covariates (90%)	6
2.4	Movement Model (80%)	7
2.5	Dispersal Simulation (80%)	9
2.6	Source Points (90%)	9
2.7	Heatmap (100%)	10
2.8	Betweenness (80%)	10
2.9	Interpatch-Connectivity (80%)	10
3	Results	11
3.1	Movement Model (20%)	11
3.2	Dispersal Simulation (60%)	12
3.3	Heatmap (50%)	12
3.4	Betweenness (50%)	13
3.5	Interpatch Connectivity (0%)	13
4	Discussion (10%)	14
5	Authors' Contributions	16
6	Data Availability	17
7	Acknowledgements	17

¹ 1 Introduction (90%)

² 1.1 Importance of Dispersal & Connectivity (90%)

³ Dispersal is defined as the movement of individuals from their natal location to the site of
⁴ first reproduction Howard (1960). It is a vital process governing the dynamics wild ani-
⁵ mal populations that are distributed in space (Hanski, 1998; Clobert et al., 2012) and may
⁶ strongly affect population dynamics at different spatial and social scales (Hanski, 1999a;
⁷ Clobert et al., 2012). Dispersal allows species to avoid inbreeding and maintain genetic di-
⁸ versity (Perrin and Mazalov, 1999, 2000; Frankham et al., 2002; Leigh et al., 2012; Baguette
⁹ et al., 2013), to rescue small and non-viable populations (Brown and Kodric-Brown, 1977),
¹⁰ and to promote the colonization of unoccupied habitats (Hanski, 1999b; MacArthur and
¹¹ Wilson, 2001). However, successful dispersal requires a sufficient degree of functional con-
¹² nectivity (Fahrig, 2003; Clobert et al., 2012), which is why the identification and protection
¹³ of major dispersal corridors has become an important task in conservation science (Doerr
¹⁴ et al., 2011; Rudnick et al., 2012). To achieve this, reliable information on movement be-
¹⁵ havior during dispersal and knowledge about factors that limit dispersal and connectivity is
¹⁶ paramount (Baguette et al., 2013; Vasudev et al., 2015).

¹⁷ 1.2 Advancements in GPS Technology & Movement Ecology (90%)

¹⁸ Thanks to novel technologies developed over the past decades, particularly of GPS/Satellite
¹⁹ radio-collars, the use of GPS data to study animal dispersal and connectivity has accelerated
²⁰ (Elliot et al., 2014; Jönsson et al., 2016; Williams et al., 2019). Additionally, the advent of
²¹ publicly accessible satellite imagery and sophisticated remote sensing techniques to represent
²² the physical landscape through which individuals disperse have heralded a “golden age
²³ of animal tracking” (Kays et al., 2015). Concurrently, the availability of large amounts
²⁴ of empirical data and an increased computational power have led to the development of
²⁵ numerous techniques to study dispersal movements and highlight critical corridors between
²⁶ subpopulations (Boyce et al., 2002; Fortin et al., 2005; Cushman and Lewis, 2010; Zeller
²⁷ et al., 2012; Diniz et al., 2020).

²⁸ 1.3 Resource Selection & Connectivity (90%)

²⁹ *Resource selection functions* (Boyce et al., 2002) and derived methods such as *step selection*
³⁰ *functions* (Fortin et al., 2005) and *path selection functions* (Cushman and Lewis, 2010) have
³¹ proven particularly useful for studying animal movement (Fieberg et al., 2020) and modelling

32 connectivity (Diniz et al., 2020). These methods allow estimating habitat preferences of the
33 focal species by comparing covariates at locations visited by the animal to the same covariates
34 at locations available to, but not visited by the animal (Boyce et al., 2002; Fortin et al., 2005;
35 Cushman and Lewis, 2010; Thurfjell et al., 2014). The so estimated preferences can then be
36 used to predict a permeability surface, indicating the expected ease at which an animal can
37 traverse a given area (Spear et al., 2010; Zeller et al., 2012; Etherington, 2016). Ultimately,
38 the permeability surface serves as input to a connectivity model that is used to reveal
39 movement corridors (Diniz et al., 2020). Two of the most prominent connectivity models
40 are least-cost path analysis (LCP analysis; Adriaensen et al., 2003) and circuit theory (CT
41 McRae, 2006; McRae et al., 2008), both graph-based methods that estimate conductance of
42 the landscape. Despite their intuitive nature and ease of use, both methods make rigorous
43 assumptions about animal movement that may or may not be fulfilled in reality (Diniz et al.,
44 2020).

45 **1.4 Issues with Least-Cost Paths & Circuit Theory (90%)**

46 In LCP analysis, for instance, a least costly path always exists, even if associated move-
47 ment costs are unreasonably high and will never be incurred by a dispersing individual.
48 The method also presumes that animals have an infinite perceptual range, a preconceived
49 end-point in mind, and choose a cost-minimizing route accordingly. These assumptions may
50 be reasonable for migrating animals, yet they are unlikely to be true for dispersers that
51 move over long distances into unknown territory (Koen et al., 2014; Abrahms et al., 2017;
52 Cozzi et al., 2020). Finally, LCPs are only one pixel wide, meaning that their absolute size
53 depends on the resolution of chosen covariate layers (Diniz et al., 2020). Although some
54 of these issues can be alleviated using less stringent versions of the LCP algorithm (e.g.
55 least-cost *corridors* (Pinto and Keitt, 2009), *thresholded* least-cost paths (Landguth et al.,
56 2012), and *randomized* least-cost paths (Panzacchi et al., 2016; Van Moorter et al., 2021)),
57 a certain degree of arbitrariness in the assumptions remains. CT entails similar restrictions.
58 Because CT only considers movements from the source cell to its 4 or 8 adjacent cells, it
59 implicitly posits a perceptual range of a single pixel. It is also built on the assumption of a
60 complete random walk (Diniz et al., 2020), implying that directional biases cannot be ren-
61 dered, albeit being very common in dispersal movements (Cozzi et al., 2020; Hofmann et al.,
62 2021). Ultimately, both LCP analysis and CT omit the temporal dimension of dispersal.
63 In result, statements about the expected duration required to traverse a certain corridor
64 are impossible. Because movement is not modelled explicitly, neither of the methods can

65 render possible interactions between movement behavior and landscape characteristics such
66 that connectivity mainly arises as a result of the landscape structure. This is referred to
67 as structural connectivity and stands in contrast to functional connectivity, which also ren-
68 ders the behavioral response of the animal with respect to prevailing habitat conditions
69 (Tischendorf and Fahrig, 2000). Even though functional connectivity is more difficult to
70 estimate, a functional view is the ultimate goal in conservation science because it has direct
71 consequences for gene flow (Baguette et al., 2013).

72 **1.5 What about IBMMS? (90%)**

73 To address the issues inherent to LCPs and CT, individual-based movement models (IBMMS)
74 have been proposed and applied (Diniz et al., 2020). In these models, dispersal is simulated
75 explicitly, based on movement rules that determine how individuals move over and interact
76 with the prevailing landscape (Kanagaraj et al., 2013; Clark et al., 2015; Allen et al., 2016;
77 Hauenstein et al., 2019; Zeller et al., 2020; Vasudev et al., 2021). Using the simulated
78 trajectories, one can calculate a set of connectivity metrics, such as interpatch-connectivity
79 and traversal frequency across the landscape to reveal major dispersal hotspots (Kanagaraj
80 et al., 2013; Bastille-Rousseau et al., 2018; Hauenstein et al., 2019; Zeller et al., 2020). Even
81 though IBMMS can be employed to overcome any of the shortcomings intrinsic to LCPs and
82 CT, as well as to provide a more functional view on connectivity, they can be challenging
83 to fit and require vast amounts of data collected during dispersal (Diniz et al., 2020).

84 **1.6 Step Selection Analysis (90%)**

85 Here, we investigate the usefulness of integrated step selection functions (ISSFs, Avgar et al.,
86 2016), as a relatively simple but powerful IBMM based on which dispersal can be simulated.
87 While regular SSFs were intended to learn about relative habitat preferences of the focal
88 species (Fortin et al., 2005; Thurfjell et al., 2014; Avgar et al., 2017), the method has been
89 generalized and now enables to jointly study habitat and movement preferences, as well as
90 potential interactions between movement and habitat preferences (Avgar et al., 2016; Signer
91 et al., 2017; Fieberg et al., 2020). ISSFs therefore provide a relatively simple method to
92 model complex movement behavior where movement results from two intertwined behavioral
93 kernels (e.g. Prokopenko et al., 2017; Munden et al., 2020). Importantly, a parametrized
94 ISSF model can be viewed as a fully mechanistic movement model based on which individual
95 movement trajectories can be simulated (Avgar et al., 2016; Signer et al., 2017). In fact,
96 Signer et al. (2017) used ISSF to simulate steady state utilization distributions of resident

97 animals. However, the degree to which such simulations are helpful in detecting movement
98 corridors and modeling landscape connectivity is unknown.

99 **1.7 Study Species & Study Area (90%)**

100 One of the species for which long-term viability relies on sufficient landscape connectivity is
101 the endangered African wild dog *Lycon pictus*. While once present across entire sub-Saharan
102 Africa, wild dogs have disappeared from a vast majority of their historic range due to per-
103 secution by humans, habitat destruction, and deadly diseases. As of today, only 6'000 free-
104 ranging individuals remain in small and spatially scattered subpopulations (Woodroffe and
105 Sillero-Zubiri, 2012). Within those subpopulations, wild dogs form cohesive packs compris-
106 ing 8 to 12 adults and their offspring McNutt (1995). After reaching sexual maturity, male
107 and female offspring form same-sex coalitions and disperse from their natal pack (McNutt,
108 1996; Behr et al., 2020). New packs are formed when dispersing coalitions join unrelated
109 opposite-sex dispersing coalitions (McNutt, 1996). Dispersing wild dogs can cover several
110 hundred kilometers across a variety of landscapes (Davies-Mostert et al., 2012; Masenga
111 et al., 2016; Cozzi et al., 2020; Hofmann et al., 2021). One of the few strongholds for this
112 species lies near the Moremi Game Reserve in northern Botswana, which is part of the
113 world's largest transboundary protected area, namely the Kavango-Zambezi Transfrontier
114 Conservation Area (KAZA-TFCA). This area has originally been intended to facilitate mi-
115 gration of elephants, but is expected to benefit a multitude of other species (Elliot et al.,
116 2014; Brennan et al., 2020; Hofmann et al., 2021).

117 **1.8 Previous Paper (90%)**

118 In a previous study, we assessed landscape connectivity for dispersing African wild dogs
119 within the KAZA-TFCA using a least-cost corridor approach (Hofmann et al., 2021). For
120 this, we fitted a basic habitat selection model based on which we predicted landscape per-
121 meability. We now expand on this knowledge and use ISSF to develop a more detailed
122 movement model of dispersing wild dogs. We then use this model to simulate dispersers
123 moving across the KAZA-TFCA. Based on simulations, we compute heatmaps and identify
124 potential dispersal hotspots. We also showcase how network metrics relevant to landscape
125 connectivity can be computed. Our results show that a simulation-based approach yields
126 several major benefits over traditional connectivity modeling techniques. Most importantly,
127 simulations provide a more generic view on how connectivity emerges and to which degree
128 connectivity depends on the dispersal duration. In addition, by generating proper dispersal

¹²⁹ trajectories, network theory can be applied to calculate network metrics that are pertinent
¹³⁰ to connectivity analysis. Finally, we put forward additional opportunities using simulations
¹³¹ that go beyond the scope of this paper.

¹³² **2 Methods**

¹³³ **2.1 Study Area (90%)**

¹³⁴ The study area was centered at -17°13'9"S, 23°56'4"E (Figure 1a) and was represented by a
¹³⁵ rectangular bounding box that stretched over 1.3 Mio. km², encompassing the entire KAZA-
¹³⁶ TFCA (Figure 1b). The KAZA-TFCA is the world's largest transboundary conservation
¹³⁷ area and comprises parts of Angola, Botswana, Namibia, Zimbabwe, and Zambia, covering a
¹³⁸ total of 520'000 km². Its landscape varies regionally and ranges from savanna, to grassland
¹³⁹ and from dry to moist woodland habitats. A dominant hydrogeographical feature in its
¹⁴⁰ center is the flood-pulsing Okavango Delta. The wet season within the KAZA-TFCA lasts
¹⁴¹ from November to March and is out of phase with the main flooding of the Okavango Delta
¹⁴² which peaks between July and August (McNutt, 1996; Wolski et al., 2017). While large
¹⁴³ portions within the KAZA-TFCA are designated national parks or other protected areas,
¹⁴⁴ substantial human influence remains due to roads, agricultural sites and settlements and
¹⁴⁵ villages.

¹⁴⁶ **2.2 GPS Relocation Data (90%)**

¹⁴⁷ Between 2011 and 2019, we collected GPS relocation data on dispersing wild dogs from a free-
¹⁴⁸ ranging wild dog population inhabiting the Moremi National Park in northern Botswana.
¹⁴⁹ We selected potential dispersers based on age, pack size, number of same-sex siblings
¹⁵⁰ within the pack, and presence of unrelated opposite-sex individuals in the pack (McNutt,
¹⁵¹ 1996; Behr et al., 2020). We immobilized selected individuals using a cocktail of Ke-
¹⁵² tamine/Xylazine/Atropine (Osofsky et al., 1996; Cozzi et al., 2020) that was injected by dart,
¹⁵³ fired from a CO₂-pressurized gun (*DAN-Inject, Denmark*). Immobilized individuals were
¹⁵⁴ fitted with GPS/Satellite radio collars (*Vertex Lite; Vectronic Aerospace GmbH, Berlin*)
¹⁵⁵ that guaranteed automated drop-off through a decomposable piece of cotton. Handling and
¹⁵⁶ collaring of all individuals was supervised by a Botswana-registered wildlife veterinarian. All
¹⁵⁷ individuals rejoined their pack within one hour after immobilization. 16 collared individuals
¹⁵⁸ eventually dispersed, each in a separate same-sex dispersal coalition (7 female and 9 male
¹⁵⁹ coalitions).

Because behavior during dispersal is more pertinent for assessing landscape connectivity (Elliot et al., 2014; Abrahms et al., 2017), we discarded all data that was collected during residency and only retained GPS data recorded during dispersal. During dispersal, collars were programmed to record a GPS fix every 4 hours. Collected relocations were regularly transmitted over the Iridium satellite system, which allowed remote tracking of individuals, even if they left the main study area and crossed international borders. In some instances, exact dispersal dates were known from field observations. Otherwise, we distinguished between residency and dispersal using the net-squared displacement metric. This metric measures the squared Euclidean distance of a GPS relocation to a reference point (Börger and Fryxell, 2012), which in our case was set to the center of each individual's natal home range. As such, dispersal was deemed to have started when an individual left its natal home range and ended once individuals became sedentary again. As previous research revealed similar behavior of females and males during dispersal (Woodroffe et al., 2019; Cozzi et al., 2020), we did not distinguish between sexes. After collection, we converted collected GPS coordinates ($n = 4'169$) to steps, where each step represented the straight-line distance traveled by an individual between two consecutive GPS relocations (Turchin, 1998). To ensure a regular sampling interval, we removed fixes that were not successfully collected on the 4-hourly schedule.

2.3 Covariates (90%)

We represented the physical landscape across the study area using a set of habitat covariates including water-cover, distance to water, woodland-cover, and shrub/grassland-cover. Because water cover greatly changes within and between years in the Okavango Delta, we applied a remote sensing algorithm and generated frequently updated water cover layers and corresponding distance to water layers (see Wolski et al., 2017 and Hofmann et al., 2021). Resulting layers thus temporally aligned with our dispersal events. We furthermore computed a proxy for human influence, depicting anthropogenic pressures stemming from human-density, agricultural sites, and roads. All spatial layers were coarsened or interpolated to a target resolution of 250 m by 250 m. Further details on the sources and preparation of each habitat covariate are given in Hofmann et al. (2021).

Besides habitat covariates, we also computed movement metrics that we used as movement covariates in our models. Movement metrics were calculated for each step and included the step length (sl), its natural logarithm ($\log(sl)$), and the cosine of the relative turning angle ($\cos(ta)$). Because wild dogs follow a diurnal activity pattern, we also coded a binary

193 variable (`LowActivity`) indicating whether a step was realized during periods of low wild dog
194 activity (17:00 to 07:00 local time) or high wild dog activity (09:00 to 17:00 local time).
195 Handling and manipulation of all data, as well as all models and simulations were imple-
196 mented with the statistical software R, version 3.6.6 (R Core Team, 2019). Several helper
197 functions were written in C++ and imported into R using the `Rcpp` package (Eddelbuettel
198 and François, 2011; Eddelbuettel, 2013)

199 **2.4 Movement Model (80%)**

200 We used ISSFs to parametrize a mechanistic movement model for dispersing wild dogs
201 (Avgar et al., 2016). To conduct iSSF analysis, we paired each observed step with 24
202 random steps. An observed and its 24 random steps thus formed a stratum and received a
203 unique identifier. We generated random steps by sampling random turning angles from a
204 uniform distribution $(-\pi, +\pi)$ and step lengths from a gamma distribution that was fitted
205 to observed steps (scale = 6'308, shape = 0.37). Along each step, we extracted and averaged
206 spatial covariates using the `velox`. We also calculated the movement metrics `sl`, `log(sl)`, and
207 `cos(ta)`. To facilitate model convergence, we standardized all continuous covariates to a
208 mean of zero and a standard deviation of one. Since correlation among covariates was low
209 ($|r| > 0.6$; Latham et al., 2011), we retained all of them for modeling.

210 To contrast realized steps (scored 1) and random steps (scored 0), we assumed that ani-
211 mals assigned a selection score $w(x)$ of the exponential form to each step. The selection score
212 $w(x)$ of each step depended on its associated covariates (x_1, x_2, \dots, x_n) and on the animal's
213 relative selection strengths (i.e. preferences) towards these covariates $(\beta_1, \beta_2, \dots, \beta_n)$:

$$w(x) = \exp(\beta_1 x_1 + \beta_2 x_2 + \dots + \beta_n x_n) \quad (\text{Equation 1})$$

214 The probability of a step being realized was then contingent on the step's selection score,
215 as well as on the selection scores of all other step in the same stratum:

$$P(Y_i = 1 | Y_1 + Y_2 + \dots + Y_i = 1) = \frac{w(x_i)}{w(x_1) + w(x_2) + \dots + w(x_i)} \quad (\text{Equation 2})$$

216 To estimate the preferences of interest, we ran conditional logistic regression models in
217 the r-package `glmmTMB`. To handle multiple individuals, we applied the mixed effects method
218 developed by (Muff et al., 2020), which allows to fit random slopes in addition to random
219 intercepts. Thus, we treated animal IDs as random effect and modeled random slopes for

220 each covariate. We fixed the random intercept variance at an arbitrary high value of 10^6 to
221 make use of the “poission”-trick (Muff et al., 2020).

222 The movement model was based on the habitat selection model for dispersing wild dogs
223 presented in Hofmann et al. (2021). In the original model, no interactions between the
224 habitat and movement covariates were considered, so we slightly expanded this base model
225 by proposing interactions between movement and habitat covariates. More specifically, we
226 started with the base model and incrementally increased model complexity by adding all
227 possible two-way interactions between habitat covariates and movement covariates. For
228 instance, for the covariate `water`, we proposed the interactions `Water:log(sl)`, `Water:log(sl)`,
229 and `Water:cos(ta)`. Besides those combinations, we also proposed the interactions `sl:cos(ta)`
230 and `log(sl):cos(ta)` to account for a correlation between turning angles and step lengths, as
231 well as the interactions `sl:LowActivity` and `log(sl):LowActivity` to account for the fact that
232 step lengths may differ due to wild dogs’ diurnal activity pattern. To compare competing
233 models and assess the most parsimonious movement model, we ran stepwise forward model
234 selection based on Akaike’s Information Criterion (AIC, Burnham and Anderson, 2002).

235 We validated the predictive power of the most parsimonious movement model using k-
236 fold cross-validation for case-control studies as presented Fortin et al. (2009). We randomly
237 split the input data into training and testing data with an 80:20 ratio. Using the training
238 data we parametrized a movement model based on which we predicted selection scores $w(x)$
239 for all steps in the test data. Within each stratum we then assigned ranks 1-25 to each step
240 based on predicted selection scores such that rank 1 was given to the step with the highest
241 score $w(x)$. Across all strata we determined the realized step’s rank and calculated rank
242 frequencies for realized steps. Finally, we computed Spearman’s rank correlation between
243 ranks and associated frequencies $r_{s,realized}$. We replicated the entire procedure 100 times
244 and computed the mean correlation coefficient ($\bar{r}_{s,realized}$), as well as its 95% confidence
245 interval across all replicates. For comparison, we repeated the same procedure 100 times
246 assuming random preferences. Random preferences were implemented by discarding the
247 realized step from all strata and identifying the rank of a random step in each stratum.
248 Again, we calculated Spearman’s rank correlation coefficient ($r_{s,random}$), its mean across
249 repetitions ($\bar{r}_{s,random}$), and its 95% confidence interval. This validation proofs a significant
250 prediction in case the confidence intervals of $\bar{r}_{s,realized}$ and $\bar{r}_{s,random}$ do not overlap.

251 **2.5 Dispersal Simulation (80%)**

252 We used the most parsimonious movement model to simulate 80'000 dispersing wild dogs
253 moving across the KAZA-TFCA. The simulation resembled an inverted iSSF and was set up
254 as follows. (1) We defined a random source point and assumed a random initial orientation of
255 the animal. (2) Departing from the source point, we generated 25 random steps by sampling
256 relative turning angles from a uniform distribution $(-\pi, +\pi)$ and step lengths from our fitted
257 gamma distribution. Each step corresponded to the straight line movement conducted within
258 4 hours. To prevent unreasonably large steps, we capped sampled values to a maximum of
259 35 km, which corresponds to the farthest distance ever traveled within 4 hours by one of
260 our dispersers. (3) Along each random step, we extracted and averaged habitat covariates
261 and calculated movement covariates. Extracted values were again standardized using the
262 same transformations that were used on the input data. (4) We applied the parameterized
263 movement model and predicted the selection score $w(x)$ for each random step and translated
264 selection scores into probabilities using Equation (Equation 2). (5) We randomly sampled
265 one of the steps based on predicted probabilities and determined the animal's new position.
266 We repeated steps (2) to (5) until a total of 2'000 steps were realized.

267 To minimize the influence of edge effects and to deal with random steps leaving the study
268 area, we followed (Koen et al., 2010) and artificially expanded all covariate layers by adding
269 a 100 km buffer zone. Within the buffer zone, we randomized covariate values by resampling
270 values from the original covariate layers. In result, simulated dispersers were able to leave
271 and reenter the main study area through this buffer zone. In cases where proposed random
272 steps transgressed the outer border of this buffer zone, we resampled transgressing steps
273 until they fully lied within the buffer.

274 **2.6 Source Points (90%)**

275 We initiated virtual dispersers at 50'000 randomly selected source points within contiguous
276 protected areas larger $> 700 \text{ km}^2$ (Figure 2a). This conforms to the average home range
277 requirement of resident wild dogs (Pomilia et al., 2015) and allowed us to remove areas
278 too small to host viable wild dog populations. By distributing source points randomly, the
279 number of source points per km^2 within protected areas was approximately equal across the
280 study area. To render potential immigrants into the study system, we placed additional
281 30'000 source points inside the buffer zone around the main study area (Figure 2b). This
282 resulted in a total of 80'000 source points, each representing the start point of an individual
283 disperser.

284 **2.7 Heatmap (100%)**

285 To identify dispersal hotspots across our study area, we created a heatmap indicating the
286 absolute frequency at which each raster-cell in the study area was visited by virtual dis-
287 persers. For this, we rasterized all simulated trajectories and tallied them into a single map.
288 If the same trajectory crossed a raster-cell twice, it was only counted once. This way, we
289 did not consider revisits and mitigated biases arising from trapped individuals that were
290 moving in circles. To achieve high performance rasterization, we used the R-package `terra`
291 (Hijmans, 2020).

292 **2.8 Betweenness (80%)**

293 To pinpoint areas of exceptional relevance for connecting remote regions in our study area,
294 we converted simulated trajectories into a network and calculated betweenness scores. For
295 this, we overlaid the study area (including the buffer) with a regular raster resolved at 5
296 x 5 km. We then used the simulated trajectories to determine all transitions occurring
297 from one raster-cell to another, as well as the frequency at which those transitions occurred.
298 This resulted in an edge-list that we translated into a weighted network using the r-package
299 `igraph` (Csardi and Nepusz, 2006). Because `igraph` handles edge weights (ω) as costs,
300 we inverted the traversal frequency in each cell by applying $\omega = \frac{\sum_i^n TraversalFrequency_i}{TraversalFrequency_i}/n$.
301 Finally, we used the weighted network to calculate betweenness scores for each raster-cell
302 in the overlaid raster. The betweenness metric indicates how often a specific raster-cell lies
303 on a shortest path between two other raster-cells and is therefore a useful metric to detect
304 movement corridors (Bastille-Rousseau et al., 2018).

305 **2.9 Interpatch-Connectivity (80%)**

306 We also assessed inter-patch connectivity between national parks in our study area. The
307 decision to focus on national parks was purely out of simplicity and the same logic could
308 easily be expanded to include other protected areas as well. To quantify inter-patch connec-
309 tivity, we computed the relative frequency at which dispersers originating from one national
310 park successfully moved into another national park. This allowed us to determine *if* and
311 *how often* dispersers moved between certain national parks. Moreover, because time was
312 explicit in our IBMM, we were able to estimate *how long* dispersers had to move to realize
313 those connections.

314 **3 Results**

315 **3.1 Movement Model (20%)**

316 Compared to the base model reported in (Hofmann et al., 2021), our most parsimonious
317 movement model included several additional interactions between habitat covariates and
318 movement covariates (Figure 3 and Table 1). Although multiple models received an AIC
319 weight above zero (Table 1 in Appendix S1), we only considered results from the most
320 parsimonious model. Since all models with positive AIC weight contained similar covariates,
321 this decision only marginally influenced subsequent results. Results from the selected model
322 are given in Table 1 and illustrated in Figure 3 (a). Additional plots that facilitate the
323 interpretation of the model are provided in Appendix S2.

324 When looking at the habitat kernel and holding constant the movement kernel, we find
325 that dispersing wild dogs avoid water but prefer its proximity. Dispersers also avoid densely
326 forested woodlands, yet prefer open shrublands or grasslands. Finally, dispersers avoid
327 moving through landscapes that are influenced by humans. These results align with our
328 previous findings reported in Hofmann et al. (2021).

329 When looking at the movement kernel, we observe several significant estimates. How-
330 ever, except for the interaction `sl:LowActivity`, effect sizes are relatively small, suggesting
331 that our proposal distributions for step lengths and turning angles were only marginally
332 biased. For instance, the positive and significant effect for `cos(ta)` indicates that realized
333 turning angles were slightly more directional than the turning angles proposed by our uni-
334 form distribution, implying that realized steps in fact followed a von Mises Distribution with
335 positive concentration parameter. On the other hand, the significant and negative interac-
336 tion for `sl:LowActivity` reveals that wild dogs moved over shorter distances during low wild
337 dog activity compared to the steps suggested by our gamma distribution.

338 Finally, we turn to the interactions between the two kernels. Here, we observe that
339 movement behavior significantly differs depending on habitat covariates. In general, steps
340 tend to be shorter in areas with high water cover and high woodland cover, yet larger in
341 areas with open shrubs and grasslands. Similarly, dispersers realized shorter steps in the
342 vicinity to water, even though the size of this effect is negligible. Finally, it appears that
343 dispersers move more tortuous in areas influenced by humans, and more directional when
344 far from water.

345 As can be seen in Figure 3b, the k-fold cross-validation procedure reveals that our model
346 substantially outperforms a random guess, as indicated by the fact that the confidence

347 intervals of $\bar{r}_{s,realized}$ and $\bar{r}_{s,random}$ do not overlap. Furthermore, the significant correlation
348 between ranks and corresponding frequencies for realized steps indicates a good fit between
349 predictions and observations (Figure 3b). Finally, we find that the rank correlation slightly
350 improved in comparison to the base model ($\bar{r}_{s,realized} = -0.55$; Hofmann et al., 2021).

351 3.2 Dispersal Simulation (60%)

352 On a machine with an AMD Ryzen 7 2700X processor with 8 x 3.6 GHz and 64 GB of
353 RAM, a single batch of 1'000 simulated dispersers took roughly 90 minutes to compute
354 ($\mu = 88.90$, $\sigma = 1.87$). As such, the simulation of all 80'000 dispersers terminated after
355 120 hours, i.e. five days. Comparable computations will be substantially quicker for smaller
356 study areas or lower resolution covariates, as the covariate extraction from large rasters was
357 computationally the most expensive task.

358 On average, step lengths realized by the simulated dispersers ($\mu_{sl} = 2'093$ m, $\sigma_{sl} =$
359 $3'067$) were slightly shorter than those by observed dispersers ($\mu_{sl} = 2'326$ m, $\sigma_{sl} = 3'323$).
360 Simultaneously, simulated dispersers moved marginally less directional ($\mu_{cos(ta)} = 0.057$,
361 $\sigma_{cos(ta)} = 0.071$) compared to observed dispersers ($\mu_{cos(ta)} = 0.078$, $\sigma_{cos(ta)} = 0.072$). These
362 differences in step lengths and turning angles can be attributed to minor disparities between
363 habitat conditions at the area within which we collected training data and habitat conditions
364 within the entire study area.

365 Out of the 50'000 dispersers initiated in protected areas, only 4.5% eventually hit a map
366 boundary, suggesting that biases due to boundary effects should be minimal. In contrast,
367 78% of the 30'000 dispersers originating from the buffer zone eventually hit a map boundary.

368 3.3 Heatmap (50%)

369 Figure 4 depicts the heatmap of all 80'000 simulated trajectories rendered after 2'000 steps.
370 The map highlights that large portions of land beyond the borders of the KAZA-TFCA are
371 only infrequently visited by dispersers (dark blue areas), whereas within the KAZA-TFCA
372 we observe several extensive regions that are regularly visited (bright yellow and red areas).
373 Most notably, the region in northern Botswana south of the Linyanti swamp stands out as
374 highly frequented dispersal hub. Still, the presence of several massive water bodies, such as
375 the Okavango Delta, the Makgadikgadi Pan, and the Linyanti swamp, results in considerable
376 dispersal barriers that limit realized connectivity within the KAZA-TFCA. Similarly, dispersal
377 appears to be very limited in Zambia's and Zimbabwe's part of the KAZA-TFCA, where
378 only few areas are traversed by dispersers, which can largely be attributed to a high human

379 influence in these regions. Outside the KAZA-TFCA, the most frequently traversed regions
380 include the areas of the Central Kalahari National Park in Botswana, the area south-west
381 of the Khaudum National Park in Namibia, and the area around the Liuwa Plains National
382 Park in Zambia.

383 **3.4 Betweenness (50%)**

384 Betweenness scores of each raster-cell the study area are presented in Figure 5. While the
385 heatmap emphasized frequently visited areas, the map of betweenness reveals rather discrete
386 dispersal corridors. As can be seen, the dispersal hotspot in northern Botswana is traversed
387 by a corridor that receives a comparably high betweenness score. This implies that the region
388 is particularly crucial for connecting other regions in the study system and hence represents
389 a proper network hub. Towards east, the corridor runs through the Chobe National Park
390 into the Hwange national park, where it branches out and further extends into the distant
391 Matusadona National Park in Zimbabwe. Northwest of the Linyanti ecosystem, the same
392 corridor expands into Angola, where it splits and finally traverses over a long stretch of
393 unprotected area into the Kafue National Park in Zambia. Several additional corridors
394 with slightly lower betweenness scores exist, yet most of them run within the boundaries of
395 the KAZA-TFCA. In general, only few corridors directly link the peripheral regions of the
396 KAZA-TFCA. For instance, there are only few corridors between the Matusadona National
397 Park in Zimbabwe and the Kafue National Park in Zimbabwe. Similarly, there are no direct
398 links between the Zimbabwean and Angolan “spikes” of the KAZA-TFCA.

399 **3.5 Interpatch Connectivity (0%)**

400 The results from the second network analysis that was focused on connectivity between
401 national parks are given in Figure 6. The map shows between which national parks direct
402 links exist and how frequent they are, as well as the average duration a disperser had to
403 move to realize those links. For instance, 6.8 % of the simulated dispersers originating from
404 the Moremi National Park successfully reached the Chobe National Park and 4.2 % reached
405 the Hwange National Park in Zimbabwe. On average, dispersers moved for 623 steps before
406 arriving at Chobe ($SD = 520$) and for 1'413 steps before arriving at Hwange ($SD = 371$).

407 4 Discussion (10%)

408 Our connectivity network further suggests that dispersers from the Okavango Delta more
409 likely disperse towards east than west. Indeed, only x out of our y observed dispersers ever
410 reached the western part of the delta. Only when the flood retracts a small pathway between
411 the city of Maun and the floodwaters of the delta emerges and enables dispersers to move
412 towards the delta's western part.

413 All of our findings are well in line with our previous work, where we have highlighted
414 dispersal corridors for wild dogs using least-cost approaches. This suggests that qualitative
415 results are quite insensitive to the exact methodological approach. Still, we believe that a
416 simulation-based approach offers possibilities for much richer inferences compared to tra-
417 ditional approaches. This is largely due to the fact that proper movement trajectories are
418 generated that can be analysed *as if* they were generated by real dispersers. This is of course
419 contingent on the assumption that underlying models are adequately representing movement
420 behavior of the focal species and calls for further methods to validate the predictive power
421 of such simulations.

422 While the segment running into Kafue receives a high betweenness score, it was actually
423 only rarely traversed by our simulated dispersers, as can be seen from the dark colors in
424 this region in Figure 4. It is therefore worth noting that the betweenness metric highlights
425 crucial bottlenecks that are relevant for connecting remote regions, yet does not directly
426 yield information about the absolute frequency at which these bottlenecks are used.

427 We have previously attributed the weak significance of distance to water to the fact that
428 we did not control for the presence or absence of conspecifics. We stick to this reasoning
429 as our expanded model still shows a rather large uncertainty around the respective beta
430 coefficients. To better gauge the importance and influence of this covariate, future studies
431 will need to control for inter- and intra-specific interactions that may explain why and when
432 dispersers are attracted to or afraid of waterbodies.

433 For our simulations, we represented the Okavango Delta statically and assumed a rela-
434 tively extended flood. This resulted in a quasi-barrier, formed by the Okavango-Delta and
435 the adjacent city of Maun, which was rarely traversed by simulated individuals. Out of
436 the 499 dispersers initiated inside the Moremi National Park, only 101 managed to reach
437 the south-western section of the Delta, whereas 284 eventually reached the equally distant
438 Linyanti swamp. In this regard, the heatmap presented in Figure 4 may be most represen-
439 tative of the period shortly after the wet-season, when floodlevels in the Delta are at their
440 maximum. During the dry season, however, the flood considerably retracts and potentially

441 clears the way for wild dogs dispersing from the Moremi-Game reserve into the south-western
442 section of the Delta. Future studies could relax the assumption of a static flood and attempt
443 to update floodlevels as the dispersers move. This would allow studying how connectivity
444 within the ecosystem evolves over time as the flood climaxes and retracts again. In fact, one
445 of the major advantages of such simulation-based approaches is that a dynamic environment
446 can be rendered, as time is explicit in these models (Zeller et al., 2020). This contrasts with
447 traditional modeling approaches such least-cost analysis or circuit theory, where the tem-
448 poral dimension cannot be made explicit. An explicit view on time also directly translates
449 in insights on the duration required by dispersers to move between distinct patches such as
450 national parks or spatially segregated subpopulations.

451 Comparable simulations that are based on empirical data are also a fundamental compo-
452 nent for spatially realistic population models in which dispersal is rendered more realistically
453 and does not merely depend on the distance between habitat patches.

454 We did not model mortality during dispersal in our simulations. This was a simplifying
455 assumption and only inaccurately reflects dispersal in reality. It is well known that wild
456 dogs often die during dispersal in result of deadly encounters with other predators, but also
457 due to road kills and illegal shootings by humans. In result, mortality during dispersal may
458 limit realized connectivity, especially in areas that wild dogs are unfamiliar with or in areas
459 with high potential for human-wildlife conflict (Cozzi et al., 2020). Interestingly though, ?
460 have recently demonstrated that mortality during dispersal is lower compared to residency,
461 suggesting the presence some fitness benefits to dispersing individuals.

462 In this regard, our approach is rather similar to dispersal kernels, yet it enables to render
463 directional biases, which are currently difficult to implement using such methods.

464 We completely randomized the location of source points within protected areas. However,
465 in some cases prior knowledge about the density of potential dispersers is available and can
466 be used to adjust the number of simulated individuals accordingly. Alternatively, instead of
467 tweaking the number of simulated individuals, one could assign a weight to each trajectory
468 that depends on the density of potential dispersers in the source areas. As such, trajectories
469 from areas with high density would enter the heatmap with above average weight.

470 The parametrized movement model could also be manipulated to investigate how differ-
471 ent habitat preferences influence landscape connectivity and to test the sensitivity of results
472 with respect to the exact preferences of individuals.

473 One of the major benefits of individual-based simulations is the ability to make the tem-
474 poral dimension of movement explicit. This allows to investigate how connectivity depends

475 on the dispersal duration, something that is not possible with traditional least-cost or circuit
476 theory methods.

477 Optimally, one should simulate additional dispersers until the amount of newly gained
478 information lies beyond a certain threshold, i.e. until some sort of convergence is achieved.
479 However, due to the myriad of outcomes in movement behavior, this would often imply
480 countless repetitions for each source points at each location where dispersal is possibly
481 initiated. This is computationally infeasible.

482 Our work suggests that the selection of source points significantly impacts resulting
483 connectivity networks. Especially when dispersal durations are short, wrongly placed source
484 points lead to vastly different results. Signer et al. used estimated utilisation distributions
485 by means of simulated movements. They used a rather long burn in period prior to alleviate
486 the problem of selecting meaningful source points. However, this approach only works when
487 individuals move around a point of attraction. This is typically not the case when simulating
488 dispersers, introducing an important trade-off. The researcher can decide to increase the
489 number of simulated steps, hence reducing the influence of starting locations, yet this also
490 inevitably increases estimated connectivity.

491 In some European countries, the comeback of large predators, such as bears, lynx, and
492 the wolf, has triggered emotional discussions and raised public concern (Behr et al., 2017),
493 particularly in areas with free-roaming livestock that may be preyed upon by the returned
494 species. In cases where recent locations of such predators are known, an early warning system
495 based on simulations could serve to forewarn about potential encounters and thereby
496 increase public acceptance of large predators.

497 Future studies could also investigate the sensitivity of such simulations with respect to
498 estimated habitat preferences. Here, we used point estimates and did not vary degree by
499 which individuals preferred or avoided certain covariates. Nevertheless, the degree to which
500 our results depend on these estimates is unknown. Because data are usually scarce for
501 dispersal studies on endangered species, point estimates may be inaccurate (Wiegand et al.,
502 2003; Kramer-Schadt et al., 2007).

503 5 Authors' Contributions

504 D.D.H., D.M.B., A.O. and G.C. conceived the study and designed methodology; D.M.B.,
505 G.C., and J.W.M. collected the data; D.D.H. and D.M.B. analysed the data; G.C. and A.O.
506 assisted with modeling; D.D.H., D.M.B., and G.C. wrote the first draft of the manuscript and
507 all authors contributed to the drafts at several stages and gave final approval for publication.

508 **6 Data Availability**

509 GPS movement data of dispersing coalitions will be made available on dryad at the time of
510 publication. Access to all R-scripts for our analyses is provided through Github.

511 **7 Acknowledgements**

512 We thank the Ministry of Environment and Tourism of Botswana for granting permission to
513 conduct this research. We thank C. Botes, I. Clavadetscher, and G. Camenisch for assisting
514 with wild dog immobilizations. We also thank B. Abrahms for sharing her data of three
515 dispersing wild dogs. Furthermore, we are indebted to Johannes Signer for assisting with the
516 simulation algorithm. This study was funded by Basler Stiftung für Biologische Forschung,
517 Claraz Foundation, Idea Wild, Jacot Foundation, National Geographic Society, Parrotia
518 Stiftung, Stiftung Temperatio, Wilderness Wildlife Trust Foundation, Forschungskredit der
519 Universität Zürich, and a Swiss National Science Foundation Grant (31003A_182286) to A.
520 Ozgul.

521 References

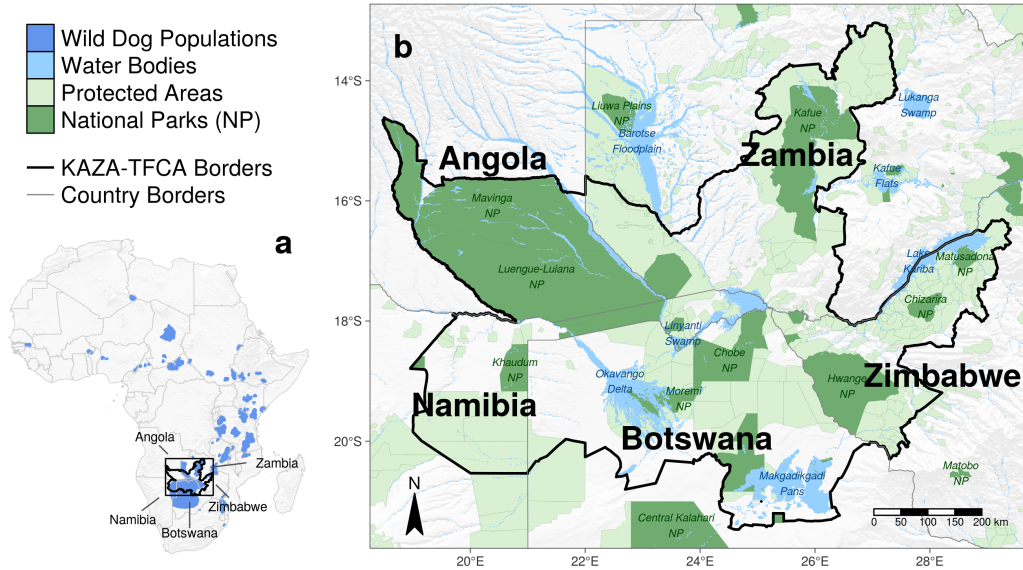
- 522 Abrahms, B., Sawyer, S. C., Jordan, N. R., McNutt, J. W., Wilson, A. M., and Brashares,
523 J. S. (2017). Does Wildlife Resource Selection Accurately Inform Corridor Conservation?
524 *Journal of Applied Ecology*, 54(2):412–422.
- 525 Adriaensen, F., Chardon, J., De Blust, G., Swinnen, E., Villalba, S., Gulinck, H., and
526 Matthysen, E. (2003). The Application of Least-Cost Modelling as a Functional Landscape
527 Model. *Landscape and Urban Planning*, 64(4):233–247.
- 528 Allen, C. H., Parrott, L., and Kyle, C. (2016). An Individual-Based Modelling Approach to
529 Estimate Landscape Connectivity for Bighorn Sheep (*Ovis canadensis*). *PeerJ*, 4:e2001.
- 530 Avgar, T., Lele, S. R., Keim, J. L., and Boyce, M. S. (2017). Relative Selection Strength:
531 Quantifying Effect Size in Habitat- and Step-Selection Inference. *Ecology and Evolution*,
532 7(14):5322–5330.
- 533 Avgar, T., Potts, J. R., Lewis, M. A., and Boyce, M. S. (2016). Integrated Step Selection
534 Analysis: Bridging the Gap Between Resource Selection and Animal Movement. *Methods
in Ecology and Evolution*, 7(5):619–630.
- 535 Baguette, M., Blanchet, S., Legrand, D., Stevens, V. M., and Turlure, C. (2013). Indi-
536 vidual Dispersal, Landscape Connectivity and Ecological Networks. *Biological Reviews*,
537 88(2):310–326.
- 538 Bastille-Rousseau, G., Douglas-Hamilton, I., Blake, S., Northrup, J. M., and Wittemyer,
539 G. (2018). Applying Network Theory to Animal Movements to Identify Properties of
540 Landscape Space Use. *Ecological Applications*, 28(3):854–864.
- 541 Behr, D. M., McNutt, J. W., Ozgul, A., and Cozzi, G. (2020). When to Stay and When
542 to Leave? Proximate Causes of Dispersal in an Endangered Social Carnivore. *Journal of
543 Animal Ecology*, 89(10):2356–2366.
- 544 Behr, D. M., Ozgul, A., and Cozzi, G. (2017). Combining Human Acceptance and Habitat
545 Suitability in a Unified Socio-Ecological Suitability Model: A Case Study of the Wolf in
546 Switzerland. *Journal of Applied Ecology*, 54(6):1919–1929.
- 547 Boyce, M. S., Vernier, P. R., Nielsen, S. E., and Schmiegelow, F. K. A. (2002). Evaluating
548 Resource Selection Functions. *Ecological Modelling*, 157(2-3):281–300.
- 549 Brennan, A., Beytell, P., Aschenborn, O., Du Preez, P., Funston, P., Hanssen, L., Kilian,
550 J., Stuart-Hill, G., Taylor, R., and Naidoo, R. (2020). Characterizing Multispecies Con-
551 nectivity Across a Transfrontier Conservation Landscape. *Journal of Applied Ecology*,
552 57:1700–1710.
- 553 Brown, J. H. and Kodric-Brown, A. (1977). Turnover Rates in Insular Biogeography: Effect
554 of Immigration on Extinction. *Ecology*, 58(2):445–449.
- 555 Burnham, K. P. and Anderson, D. R. (2002). *Model Selection and Multimodel Inference: A
556 Practical Information-Theoretic Approach*. Springer Science & Business Media, Ney York,
557 NY, USA.
- 558 Börger, L. and Fryxell, J. (2012). Quantifying Individual Differences in Dispersal Using Net
559 Squared Displacement. In Clobert, J., Baguette, M., Benton, T. G., and Bullock, J. M.,
560 editors, *Dispersal Ecology and Evolution*. Oxford University Press, Oxford, UK.
- 561 Clark, J. D., Laufenberg, J. S., Davidson, M., and Murrow, J. L. (2015). Connectivity among
562 Subpopulations of Louisiana Black Bears as Estimated by a Step Selection Function. *The
563 Journal of Wildlife Management*, 79(8):1347–1360.
- 564 Clobert, J., Baguette, M., Benton, T. G., and Bullock, J. M. (2012). *Dispersal Ecology and
565 Evolution*. Oxford University Press, Oxford, UK.

- 567 Cozzi, G., Behr, D., Webster, H., Claase, M., Bryce, C., Modise, B., McNutt, J., and
 568 Ozgul, A. (2020). The Walk of Life: African Wild Dog Dispersal and its Implications for
 569 Management and Conservation across Transfrontier Landscapes. In press.
- 570 Csardi, G. and Nepusz, T. (2006). The igraph Software Package for Complex Network
 571 Research. *InterJournal, Complex Systems*:1695.
- 572 Cushman, S. A. and Lewis, J. S. (2010). Movement Behavior Explains Genetic Differentiation
 573 in American Black Bears. *Landscape Ecology*, 25(10):1613–1625.
- 574 Davies-Mostert, H. T., Kamler, J. F., Mills, M. G. L., Jackson, C. R., Rasmussen, G. S. A.,
 575 Groom, R. J., and Macdonald, D. W. (2012). Long-Distance Transboundary Dispersal
 576 of African Wild Dogs among Protected Areas in Southern Africa. *African Journal of
 577 Ecology*, 50(4):500–506.
- 578 Diniz, M. F., Cushman, S. A., Machado, R. B., and De Marco Júnior, P. (2020). Landscape
 579 Connectivity Modeling from the Perspective of Animal Dispersal. *Landscape Ecology*.
- 580 Doerr, V. A. J., Barrett, T., and Doerr, E. D. (2011). Connectivity, Dispersal Behaviour
 581 and Conservation under Climate Change: A Response to Hodgson et al.: Connectivity
 582 and Dispersal Behaviour. *Journal of Applied Ecology*, 48(1):143–147.
- 583 Eddelbuettel, D. (2013). *Seamless R and C++ Integration with Rcpp*. Springer, New York.
 584 ISBN 978-1-4614-6867-7.
- 585 Eddelbuettel, D. and François, R. (2011). Rcpp: Seamless R and C++ Integration. *Journal
 586 of Statistical Software*, 40(8):1–18.
- 587 Elliot, N. B., Cushman, S. A., Macdonald, D. W., and Loveridge, A. J. (2014). The Devil
 588 is in the Dispersers: Predictions of Landscape Connectivity Change with Demography.
 589 *Journal of Applied Ecology*, 51(5):1169–1178.
- 590 Etherington, T. R. (2016). Least-Cost Modelling and Landscape Ecology: Concepts, Appli-
 591 cations, and Opportunities. *Current Landscape Ecology Reports*, 1(1):40–53.
- 592 Fahrig, L. (2003). Effects of Habitat Fragmentation on Biodiversity. *Annual Review of
 593 Ecology, Evolution, and Systematics*, 34(1):487–515.
- 594 Fieberg, J., Signer, J., Smith, B., and Avgar, T. (2020). A ‘How-to’ Guide for Interpreting
 595 Parameters in Resource- and Step-Selection Analyses. preprint, Ecology.
- 596 Fortin, D., Beyer, H. L., Boyce, M. S., Smith, D. W., Duchesne, T., and Mao, J. S. (2005).
 597 Wolves Influence Elk Movements: Behavior Shapes a Trophic Cascade in Yellowstone
 598 National Park. *Ecology*, 86(5):1320–1330.
- 599 Fortin, D., Fortin, M.-E., Beyer, H. L., Duchesne, T., Courant, S., and Dancose, K. (2009).
 600 Group-Size-Mediated Habitat Selection and Group Fusion–Fission Dynamics of Bison
 601 under Predation Risk. *Ecology*, 90(9):2480–2490.
- 602 Frankham, R., Briscoe, D. A., and Ballou, J. D. (2002). *Introduction to Conservation
 603 Genetics*. Cambridge University Press, Cambridge, UK.
- 604 Hanski, I. (1998). Metapopulation Dynamics. *Nature*, 396(6706):41–49.
- 605 Hanski, I. (1999a). Habitat Connectivity, Habitat Continuity, and Metapopulations in Dy-
 606 namic Landscapes. *Oikos*, 87(2):209.
- 607 Hanski, I. (1999b). *Metapopulation Ecology*. Oxford University Press.
- 608 Hauenstein, S., Fattebert, J., Grüebler, M. U., Naef-Daenzer, B., Pe'er, G., and Hartig, F.
 609 (2019). Calibrating an Individual-Based Movement Model to Predict Functional Connec-
 610 tivity for Little Owls. *Ecological Applications*, 29(4):e01873.

- 611 Hijmans, R. J. (2020). *raster: Geographic Data Analysis and Modeling*. R package version
 612 3.3-13.
- 613 Hofmann, D. D., Behr, D. M., McNutt, J. W., Ozgul, A., and Cozzi, G. (2021). Bound
 614 within Boundaries: How Well Do Protected Areas Match Movement Corridors of their
 615 Most Mobile Protected Species? *Journal of Applied Ecology*. (in 2nd review).
- 616 Howard, W. E. (1960). Innate and Environmental Dispersal of Individual Vertebrates.
 617 *American Midland Naturalist*, 63(1):152.
- 618 Jönsson, K. A., Tøttrup, A. P., Borregaard, M. K., Keith, S. A., Rahbek, C., and Thorup, K.
 619 (2016). Tracking Animal Dispersal: From Individual Movement to Community Assembly
 620 and Global Range Dynamics. *Trends in Ecology & Evolution*, 31(3):204–214.
- 621 Kanagaraj, R., Wiegand, T., Kramer-Schadt, S., and Goyal, S. P. (2013). Using Individual-
 622 Based Movement Models to Assess Inter-Patch Connectivity for Large Carnivores in Frag-
 623 mented Landscapes. *Biological Conservation*, 167:298 – 309.
- 624 Kays, R., Crofoot, M. C., Jetz, W., and Wikelski, M. (2015). Terrestrial Animal Tracking
 625 as an Eye on Life and Planet. *Science*, 348(6240):aaa2478 – aaa2478.
- 626 Koen, E. L., Bowman, J., Sadowski, C., and Walpole, A. A. (2014). Landscape Connectivity
 627 for Wildlife: Development and Validation of Multispecies Linkage Maps. *Methods in
 628 Ecology and Evolution*, 5(7):626–633.
- 629 Koen, E. L., Garraway, C. J., Wilson, P. J., and Bowman, J. (2010). The Effect of Map
 630 Boundary on Estimates of Landscape Resistance to Animal Movement. *PLOS ONE*,
 631 5(7):e11785.
- 632 Kramer-Schadt, S., Revilla, E., Wiegand, T., and Grimm, V. (2007). Patterns for Parameters
 633 in Simulation Models. *Ecological Modelling*, 204(3-4):553–556.
- 634 Landguth, E. L., Hand, B. K., Glassy, J., Cushman, S. A., and Sawaya, M. A. (2012). UNICOR:
 635 A Species Connectivity and Corridor Network Simulator. *Ecography*, 35(1):9–
 636 14.
- 637 Latham, A. D. M., Latham, M. C., Boyce, M. S., and Boutin, S. (2011). Movement Re-
 638 sponses by Wolves to Industrial Linear Features and Their Effect on Woodland Caribou
 639 in Northeastern Alberta. *Ecological Applications*, 21(8):2854–2865.
- 640 Leigh, K. A., Zenger, K. R., Tammen, I., and Raadsma, H. W. (2012). Loss of Genetic
 641 Diversity in an Outbreeding Species: Small Population Effects in the African Wild Dog
 642 (*Lycaon pictus*). *Conservation Genetics*, 13(3):767–777.
- 643 MacArthur, R. H. and Wilson, E. O. (2001). *The Theory of Island Biogeography*, volume 1.
 644 Princeton University Press, Princeton, New Jersey, USA.
- 645 Masenga, E. H., Jackson, C. R., Mjingo, E. E., Jacobson, A., Riggio, J., Lyamuya, R. D.,
 646 Fyumagwa, R. D., Borner, M., and Røskift, E. (2016). Insights into Long-Distance
 647 Dispersal by African Wild Dogs in East Africa. *African Journal of Ecology*, 54(1):95–98.
- 648 McNutt, J. (1996). Sex-Biased Dispersal in African Wild Dogs (*Lycaon pictus*). *Animal
 649 Behaviour*, 52(6):1067–1077.
- 650 McNutt, J. W. (1995). *Sociality and Dispersal in African Wild Dogs, Lycaon pictus*. PhD
 Thesis, University of California, Davis.
- 652 McRae, B. H. (2006). Isolation by Resistance. *Evolution*, 60(8):1551–1561.
- 653 McRae, B. H., Dickson, B. G., Keitt, T. H., and Shah, V. B. (2008). Using Circuit Theory to
 654 Model Connectivity in Ecology, Evolution, and Conservation. *Ecology*, 89(10):2712–2724.

- 655 Muff, S., Signer, J., and Fieberg, J. (2020). Accounting for Individual-Specific Variation in
 656 Habitat-Selection Studies: Efficient Estimation of Mixed-Effects Models Using Bayesian
 657 or Frequentist Computation. *Journal of Animal Ecology*, 89(1):80–92.
- 658 Munden, R., Börger, L., Wilson, R. P., Redcliffe, J., Brown, R., Garel, M., and Potts, J. R.
 659 (2020). Why Did the Animal Turn? Time-Varying Step Selection Analysis for Inference
 660 Between Observed Turning Points in High Frequency Data.
- 661 Osofsky, S. A., McNutt, J. W., and Hirsch, K. J. (1996). Immobilization of Free-Ranging
 662 African Wild Dogs (*Lycaon pictus*) Using a Ketamine/Xylazine/Atropine Combination.
 663 *Journal of Zoo and Wildlife Medicine*, pages 528–532.
- 664 Panzacchi, M., Van Moorter, B., Strand, O., Saerens, M., Kivimäki, I., St. Clair, C. C.,
 665 Herfindal, I., and Boitani, L. (2016). Predicting the Continuum Between Corridors and
 666 Barriers to Animal Movements Using Step Selection Functions and Randomized Shortest
 667 Paths. *Journal of Animal Ecology*, 85(1):32–42.
- 668 Perrin, N. and Mazalov, V. (1999). Dispersal and Inbreeding Avoidance. *The American
 669 Naturalist*, 154(3):282–292.
- 670 Perrin, N. and Mazalov, V. (2000). Local Competition, Inbreeding, and the Evolution of
 671 Sex-Biased Dispersal. *The American Naturalist*, 155(1):116–127.
- 672 Pinto, N. and Keitt, T. H. (2009). Beyond the Least-Cost Path: Evaluating Corridor
 673 Redundancy Using a Graph-Theoretic Approach. *Landscape Ecology*, 24(2):253–266.
- 674 Pomilia, M. A., McNutt, J. W., and Jordan, N. R. (2015). Ecological Predictors of African
 675 Wild Dog Ranging Patterns in Northern Botswana. *Journal of Mammalogy*, 96(6):1214–
 676 1223.
- 677 Prokopenko, C. M., Boyce, M. S., and Avgar, T. (2017). Characterizing Wildlife Behavioural
 678 Responses to Roads Using Integrated Step Selection Analysis. *Journal of Applied Ecology*,
 679 54(2):470–479.
- 680 R Core Team (2019). *R: A Language and Environment for Statistical Computing*. R Foun-
 681 dation for Statistical Computing, Vienna, Austria.
- 682 Rudnick, D., Ryan, S., Beier, P., Cushman, S., Dieffenbach, F., Epps, C., Gerber, L., Hart-
 683 ter, J., Jenness, J., Kintsch, J., Merenlender, A., Perkl, R., Perziosi, D., and Trombulack,
 684 S. (2012). The Role of Landscape Connectivity in Planning and Implementing Conserva-
 685 tion and Restoration Priorities. *Issues in Ecology*.
- 686 Signer, J., Fieberg, J., and Avgar, T. (2017). Estimating Utilization Distributions from
 687 Fitted Step-Selection Functions. *Ecosphere*, 8(4):e01771.
- 688 Spear, S. F., Balkenhol, N., Fortin, M.-J., Mcrae, B. H., and Scribner, K. (2010). Use of
 689 Resistance Surfaces for Landscape Genetic Studies: Considerations for Parameterization
 690 and Analysis. *Molecular Ecology*, 19(17):3576–3591.
- 691 Thurfjell, H., Ciuti, S., and Boyce, M. S. (2014). Applications of Step-Selection Functions
 692 in Ecology and Conservation. *Movement Ecology*, 2(4).
- 693 Tischendorf, L. and Fahrig, L. (2000). On the Usage and Measurement of Landscape Con-
 694 nectivity. *Oikos*, 90(1):7–19.
- 695 Turchin, P. (1998). *Quantitative Analysis of Movement: Measuring and Modeling Population
 696 Redistribution in Plants and Animals*. Sinauer Associates, Sunderland, MA, USA.
- 697 Van Moorter, B., Kivimäki, I., Panzacchi, M., and Saerens, M. (2021). Defining and Quan-
 698 tifying Effective Connectivity of Landscapes for Species' Movements. *Ecography*, page
 699 ecog.05351.

- 700 Vasudev, D., Fletcher, R. J., Goswami, V. R., and Krishnadas, M. (2015). From Disper-
701 sal Constraints to Landscape Connectivity: Lessons from Species Distribution Modeling.
702 *Ecography*, 38(10):967–978.
- 703 Vasudev, D., Goswami, V. R., and Oli, M. K. (2021). Detecting Dispersal: A Spatial Dy-
704 namic Occupancy Model to Reliably Quantify Connectivity across Heterogeneous Con-
705 servation Landscapes. *Biological Conservation*, 253:108874.
- 706 Wiegand, T., Jeltsch, F., Hanski, I., and Grimm, V. (2003). Using Pattern-Oriented Mod-
707 eling for Revealing Hidden Information: A Key for Reconciling Ecological Theory and
708 Application. *Oikos*, 100(2):209–222.
- 709 Williams, H. J., Taylor, L. A., Benhamou, S., Bijleveld, A. I., Clay, T. A., Grissac, S.,
710 Demšar, U., English, H. M., Franconi, N., Gómez-Laich, A., Griffiths, R. C., Kay, W. P.,
711 Morales, J. M., Potts, J. R., Rogerson, K. F., Rutz, C., Spelt, A., Trevail, A. M., Wilson,
712 R. P., and Börger, L. (2019). Optimizing the Use of Biologgers for Movement Ecology
713 Research. *Journal of Animal Ecology*.
- 714 Wolski, P., Murray-Hudson, M., Thito, K., and Cassidy, L. (2017). Keeping it Simple:
715 Monitoring Flood Extent in Large Data-Poor Wetlands Wsing MODIS SWIR Data. *In-*
716 *ternational Journal of Applied Earth Observation and Geoinformation*, 57:224–234.
- 717 Woodroffe, R., Rabaiotti, D., Ngatia, D. K., Smallwood, T. R. C., Strelbel, S., and O'Neill,
718 H. M. K. (2019). Dispersal Behaviour of African Wild Dogs in Kenya. *African Journal*
719 *of Ecology*.
- 720 Woodroffe, R. and Sillero-Zubiri, C. (2012). *Lycaon pictus*. *The IUCN Red List of Threatened*
721 *Species*, 2012:e. T12436A16711116.
- 722 Zeller, K. A., McGarigal, K., and Whiteley, A. R. (2012). Estimating Landscape Resistance
723 to Movement: A Review. *Landscape Ecology*, 27(6):777–797.
- 724 Zeller, K. A., Wattles, D. W., Bauder, J. M., and DeStefano, S. (2020). Forecasting Seasonal
725 Habitat Connectivity in a Developing Landscape. *Land*, 9(7):233.



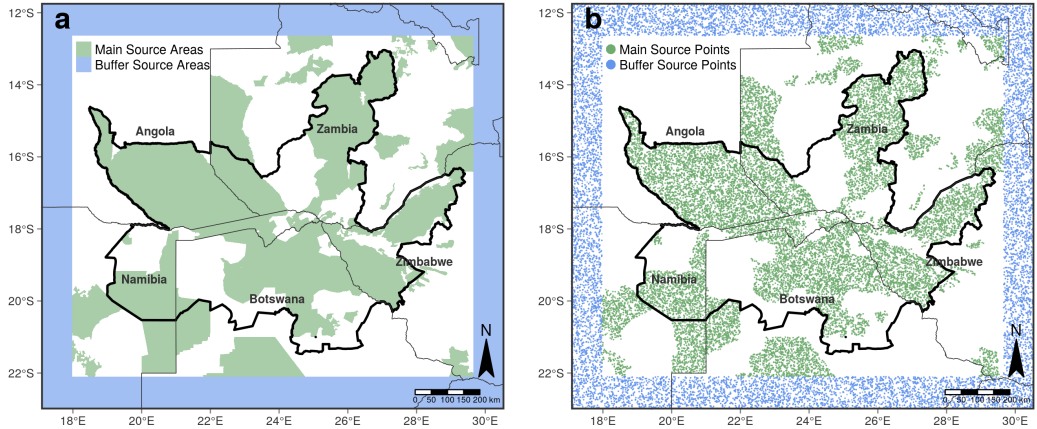


Figure 2: (a) Different source areas from which we released virtual dispersers. We only considered contiguous protected areas (national parks, game reserves, and forest reserves) that were larger than 700 km^2 (green). This area corresponds to the average home range requirement for viable wild dog populations (Pomilia et al., 2015). To render potential immigrants into the study system, we also initiated dispersers within a buffer zone (blue) surrounding the main study area. (b) Source points from which dispersers were released. 50'000 dispersers were released from the main study area (green dots) and another 30'000 dispersers within the virtual buffer (blue dots).

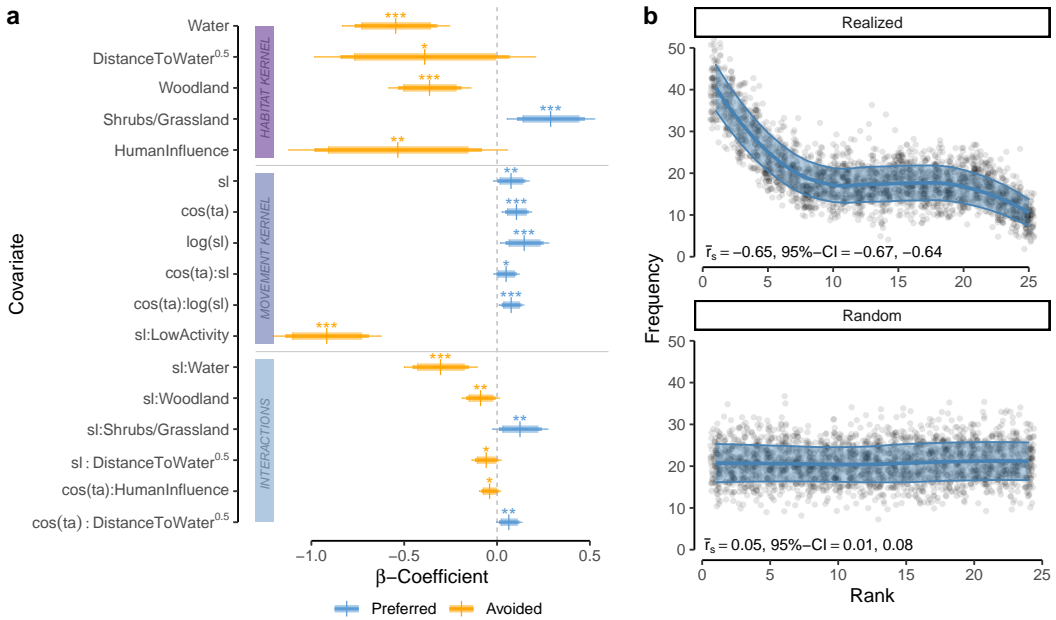


Figure 3: (a) Most parsimonious movement model for dispersing wild dogs. The model includes a habitat kernel, a movement kernel, as well as their interactions. The orange and blue line segments delineate the 90%, 95%, and 99% Confidence-Intervals around the respective β coefficients. Significance codes: * $p < 0.10$, ** $p < 0.05$, *** $p < 0.01$. (b) Results from the k-fold cross validation procedure. The upper plot shows rank frequencies of predicted realized scores according to model predictions with known preferences, whereas the lower plot shows rank frequencies when assuming random preferences. The blue ribbon shows the prediction interval around a loess smoothing regression that we fitted to ease the interpretation of the plots.

Dispersal Heatmap

After 2000 Steps

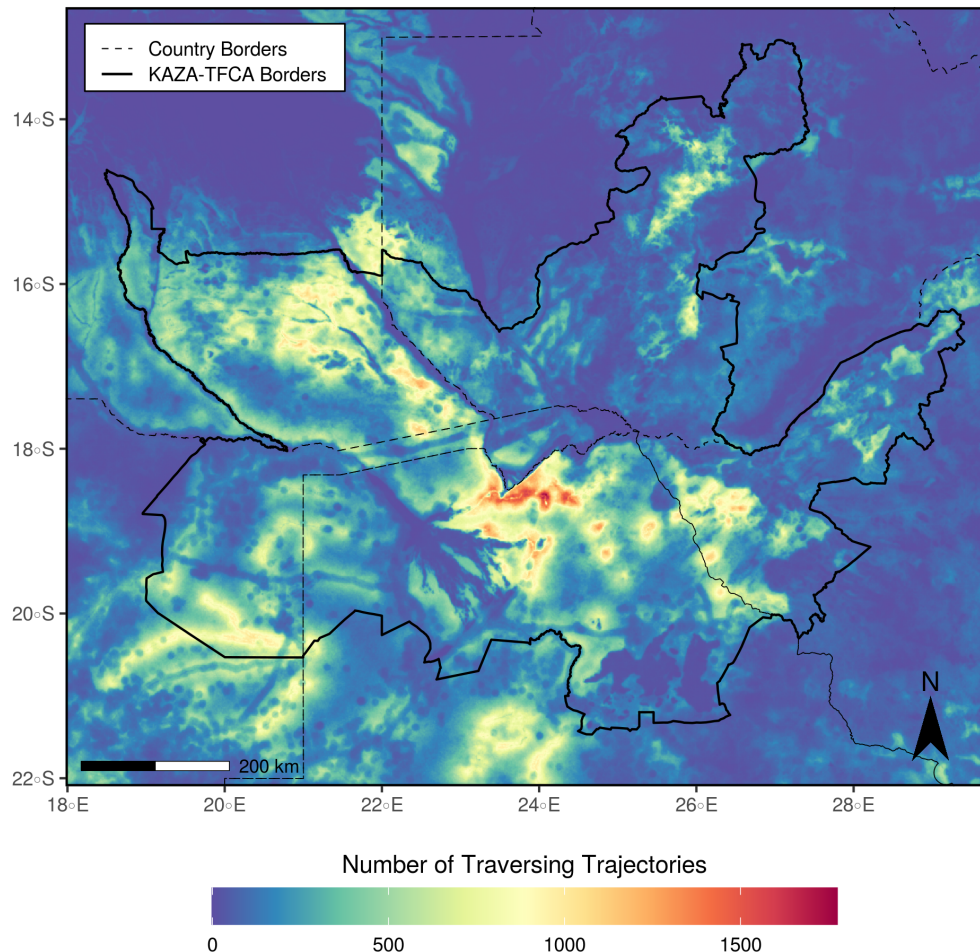


Figure 4: Heatmap of all 80'000 simulated trajectories after 2'000 steps. Simulations were based on an integrated step selection model, fit to the movement data of dispersing African wild dogs. To generate the heatmap, we rasterized and summed all simulated trajectories. Additional heatmaps showcasing the traversal frequency after different numbers of steps are provided in xx in Appendix S3.

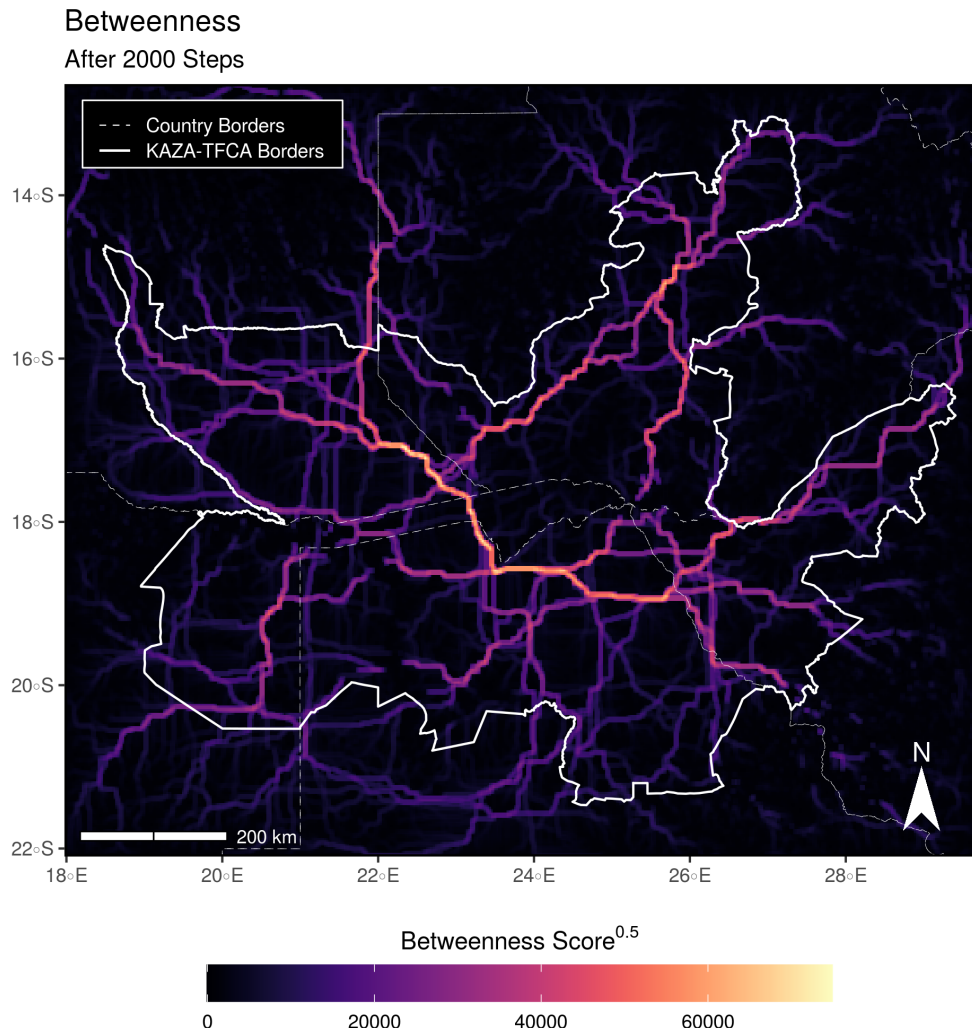


Figure 5: Betweenness scores of each raster cell in a raster with 5×5 km resolution. Betweenness scores were determined based on simulated dispersal events. A high betweenness score highlights cells that are exceptionally relevant in connecting different regions in the study area. That is, the higher the betweenness score, the more often a pixel lies on a shortest path between adjacent areas. In this sense the metric can be used to pinpoint discrete movement corridors. Note that we square-rooted betweenness scores to improve visibility of corridors with low scores.

Areas Reached and Visitation Frequency

In Relation to Number of Steps

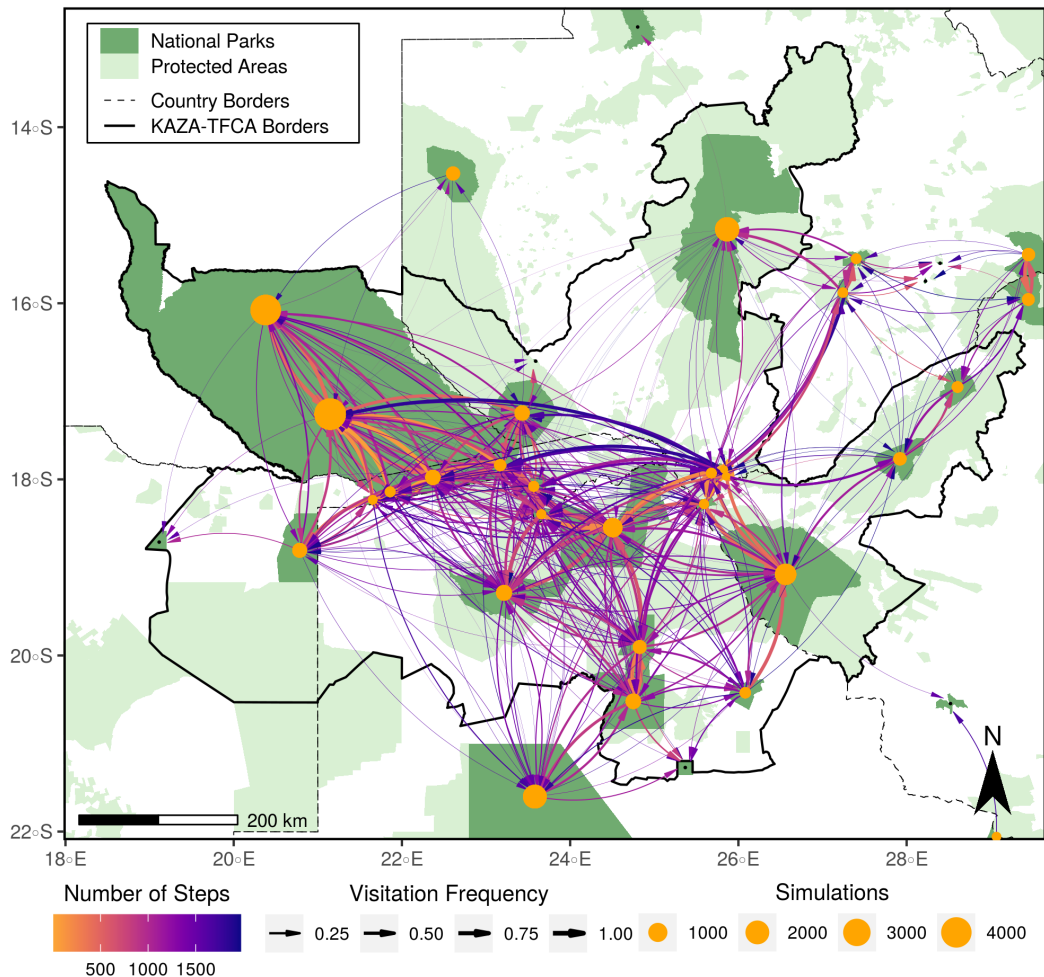


Figure 6: Network on simulated dispersal trajectories highlighting the connections between national parks (dark green). Yellow bubbles represent the center of the different national parks and are sized in relation to the number of simulated dispersers originating from each park. Colored arrows between national parks illustrate between which national parks the simulated dispersers successfully moved and the color of each arrow shows the average number of steps that were necessary to realize those connections. Additionally, the line thickness indicates the relative number of dispersers originating from a national park that realized those connections.

Table 1: Most parsimonious movement model for dispersing wild dogs. The model comprises of a movement and habitat kernel, where the movement kernels describes preferences with regards to movement behavior, whereas the habitat kernel describes preferences with respect to the habitat. Finally, the two kernels can interact, such that movement preferences are contingent on habitat conditions.

Kernel	Covariate	Coefficient	SE	p-value	Sign.
Habitat Kernel	Water	-0.546	0.112	< 0.001	***
	DistanceToWater $^{0.5}$	-0.390	0.231	0.092	*
	Woodland	-0.364	0.086	< 0.001	***
	Shrubs/Grassland	0.288	0.092	0.002	***
	HumanInfluence	-0.535	0.229	0.019	**
Movement Kernel	sl	0.075	0.037	0.042	**
	cos(ta)	0.105	0.031	0.001	***
	log(sl)	0.146	0.051	0.004	***
	cos(ta) : sl	0.049	0.026	0.064	*
	cos(ta) : log(sl)	0.076	0.026	0.003	***
Interaction	sl : LowActivity	-0.917	0.113	< 0.001	***
	sl : Water	-0.305	0.076	< 0.001	***
	sl : Woodland	-0.089	0.039	0.023	**
	sl : Shrubs/Grassland	0.124	0.058	0.032	**
	sl : DistanceToWater $^{0.5}$	-0.058	0.031	0.056	*
		cos(ta) : HumanInfluence	-0.040	0.022	0.070
		cos(ta) : DistanceToWater $^{0.5}$	0.063	0.026	0.017

Significance codes: * $p < 0.10$ ** $p < 0.05$ *** $p < 0.01$